HHS Public Access

Author manuscript

Cell Rep. Author manuscript; available in PMC 2021 December 29.

Published in final edited form as:

Cell Rep. 2021 December 07; 37(10): 110075. doi:10.1016/j.celrep.2021.110075.

Hypothalamic steroid receptor coactivator-2 regulates adaptations to fasting and overnutrition

Yongjie Yang[1,*], **Yanlin He**[1,5], **Hailan Liu**[1], **Wenjun Zhou**[2], **Chunmei Wang**[1], **Pingwen Xu**[1,6], **Xing Cai**[1,7], **Hesong Liu**[1], **Kaifan Yu**[1], **Zhou Pei**[1], **Ilirjana Hyseni**[1], **Makoto Fukuda**[1], **Qingchun Tong**[3], **Jianming Xu**[4], **Zheng Sun**[2,4], **Bert W. O'Malley**[4], **Yong Xu**[1,4,8,*]

[1]Children's Nutrition Research Center, Department of Pediatrics, Baylor College of Medicine, Houston, TX 77030, USA

[2]Department of Medicine, Baylor College of Medicine, One Baylor Plaza, Houston, TX 77030, USA

[3]Brown Foundation Institute of Molecular Medicine, University of Texas Health Science Center at Houston, Houston, TX 77030, USA

[4]Department of Molecular and Cellular Biology, Baylor College of Medicine, One Baylor Plaza, Houston, TX 77030, USA

[5]Present address: Pennington Biomedical Research Center, Brain Glycemic and Metabolism Control Department, Louisiana State University, Baton Rouge, LA 70808, USA

[6]Present address: Division of Endocrinology, Department of Medicine, the University of Illinois at Chicago, Chicago, IL 60612, USA

[7]Present address: State Key Laboratory of Genetic Resources and Evolution, Kunming Institute of Zoology, Chinese Academy of Sciences, Kunming 650223, Yunnan, China

[8]Lead contact

SUMMARY

The neuroendocrine system coordinates metabolic and behavioral adaptations to fasting, including reducing energy expenditure, promoting counterregulation, and suppressing satiation and anxiety to engage refeeding. Here, we show that steroid receptor coactivator-2 (SRC-2) in pro-opiomelanocortin (POMC) neurons is a key regulator of all these responses to fasting.

*Correspondence: yongjiey@bcm.edu (Y.Y.), yongx@bcm.edu (Y.X.).

AUTHOR CONTRIBUTIONS

Y.Y. was involved in experimental design and most procedures, data acquisition, and analyses and writing the manuscript. Y.H. assisted in electrophysiological recordings, and Hailan Liu helped with histology studies. C.W. and W.Z. helped with the behavioral experiments. P.X., X.C., Hesong Liu, K.Y., Z.P., I.H., and J.X. assisted in production of experimental mice, surgical procedures, and blinded evaluation of mouse behaviors. Z.S., M.F., Q.T., and B.W.O. were involved in study design and editing the manuscript. Y.Y. and Y.X. are the guarantors of this work and, as such, had full access to all the data in the study and take responsibility for the integrity of the data and the accuracy of the data analysis.

DECLARATION OF INTERESTS

The authors declare no competing interests.

SUPPLEMENTAL INFORMATION

Supplemental information can be found online at https://doi.org/10.1016/j.celrep.2021.110075.

POMC-specific deletion of SRC-2 enhances the basal excitability of POMC neurons; mutant mice fail to efficiently suppress energy expenditure during food deprivation. SRC-2 deficiency blunts electric responses of POMC neurons to glucose fluctuations, causing impaired counterregulation. When food becomes available, these mutant mice show insufficient refeeding associated with enhanced satiation and discoordination of anxiety and food-seeking behavior. SRC-2 coactivates Forkhead box protein O1 (FoxO1) to suppress POMC gene expression. POMC-specific deletion of SRC-2 protects mice from weight gain induced by an obesogenic diet feeding and/or FoxO1 overexpression. Collectively, we identify SRC-2 as a key molecule that coordinates multifaceted adaptive responses to food shortage.

In brief

Yang et al. demonstrate that SRC-2 in POMC neurons coordinates multifaceted adaptive responses to food shortage, including reducing energy expenditure, promoting counterregulation and suppressing satiation and anxiety to engage refeeding. These effects are mediated by SRC-2 functions to regulate POMC gene expression and modulate POMC neuron activities.

Graphical Abstract

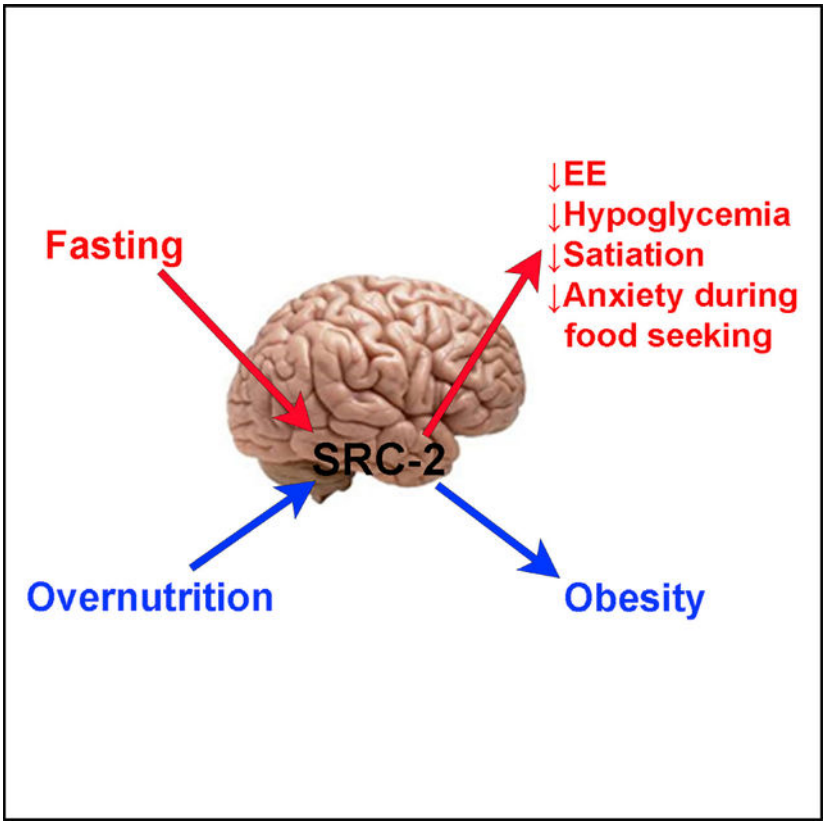

INTRODUCTION

During the course of evolution, animals (including humans) are often challenged by periods of food shortage. Upon food deprivation, the neuroendocrine system coordinates enormous

metabolic and behavioral adaptations to help ensure animal's survival (Ahima et al., 1996). These include suppression of energy expenditure to preserve energy (Vella et al., 2011), prevention of severe hypoglycemia to keep the brain nourished and alert (Romere et al., 2016), reducing anxiety and fear to facilitate searching for food that may be associated with danger (Alhadeff et al., 2018; Burnett et al., 2016; Dietrich et al., 2015; Padilla et al., 2016), and suppression of satiation to ensure efficient refeeding when food becomes available again (Duerrschmid et al., 2017).

The hypothalamus integrates information regarding the body's nutritional status and orchestrates endocrine and behavioral responses to maintain energy homeostasis (Elmquist et al., 1999; Hetherington and Ranson, 1940; Morton et al., 2006). In particular, pro-opiomelanocortin (POMC) neurons in the arcuate nucleus of hypothalamus (ARH) have been identified as the first-order neurons that respond to multiple hormonal and nutritional signals to regulate energy and glucose metabolism (Caron et al., 2018; Kim et al., 2014; Varela and Horvath, 2012). Genetic ablation of POMC neurons in the ARH leads to hyperphagia and obesity in mice (Xu et al., 2005; Zhan et al., 2013). POMC gene deficiency causes massive obesity in mice (Yaswen et al., 1999) and in humans (Challis et al., 2002; Creemers et al., 2008; Farooqi et al., 2006). On the other hand, hyperactivity of ARH POMC neurons results in hypophagia and body weight loss (Zhan et al., 2013). These findings indicate that normal POMC gene expression and POMC neuron activity are fundamentally required to maintain normal energy balance. Importantly, the excitability of POMC neurons can be inhibited by food deprivation (Yang et al., 2011); the expression of the POMC gene itself is dramatically suppressed by fasting (Ahima et al., 1999; Hillebrand et al., 2002). However, the roles of POMC neurons in coping with food deprivation are not fully understood.

Steroid receptor coactivator-2 (SRC-2) belongs to a family of nuclear receptor coactivators that regulate the ability of nuclear receptors and transcription factors to modulate target gene expression (Johnson and O'Malley, 2012; York and O'Malley, 2010). SRC-2 mediates energy adaptations through its actions in various peripheral tissues, e.g., liver (Chopra et al., 2008, 2011), fat (Picard et al., 2002), and muscle (Duteil et al., 2010). In the brain, SRC-2 is expressed in the ARH, ventromedial hypothalamic nucleus (VMH), medial preoptic area, bed nucleus of the stria terminalis, supraoptic nucleus, and suprachiasmatic nucleus (Yore et al., 2010), including hypothalamic neurons expressing progesterone receptors (Tognoni et al., 2011). However, SRC-2's functions in the brain are not clear. In the present study, we examined the functions of SRC-2 in POMC neurons in various metabolic and behavioral adaptations during the fasting-refeeding transition, delineated mechanisms by which SRC-2 regulates POMC neuron activity and POMC gene expression, and explored the roles of SRC-2 in the regulation of energy balance in the face of overnutrition challenge.

RESULTS

SRC-2 in POMC neurons suppresses energy expenditure during fasting

We found that abundant SRC-2 is expressed by a number of neural subpopulations within the ARH and VMH, including neurons expressing POMC, Agouti-related peptide (AgRP), tyrosine hydroxylase (TH), or estrogen receptor-α (Figures 1A and S1A–S1C). The present

study focused on the physiological functions of SRC-2 in POMC neurons. To this end, we generated pomcSRC-2-knockout (KO) mice lacking SRC-2 selectively in POMC neurons (Figures 1A, S1D, and S1E). When fed regular chow *ad libitum*, pomcSRC-2-KO mice displayed comparable body weight and fat or lean mass as their control littermates (Figures S2A and S2B). Interestingly, after a 24-h fasting, pomcSRC-2-KO mice lost significantly more body weight and fat storage than controls (Figures 1B, 1C, and S2C). We then adapted a cohort of body-weight-matched mice into the Comprehensive Laboratory Animal Monitoring System (CLAMS) metabolic cages and subjected them to a 3-day protocol with 24-h feed *ad libitum*, 24-h fast, and 24-h refeed. Although control mice responded to fasting with significant reductions in energy expenditure, this fasting-induced suppression in energy expenditure was significantly attenuated in pomcSRC-2-KO mice (Figures 1D, S2D, and S2E). Energy expenditure during the *ad libitum* feeding and refeeding conditions was not different between the two genotypes (Figures 1D, S2D, and S2E). Thus, these results indicate that loss of SRC-2 in POMC neurons impaired animal's capability to suppress energy expenditure during food deprivation, which accounted for the bigger body weight loss observed in these mice.

To reveal the cellular mechanisms by which SRC-2 in POMC neurons regulates energy balance, we then compared the electrophysiological properties of POMC neurons (labeled by the POMC-EGFP allele; Figure 1E) in fasted control versus pomcSRC-2-KO mice. We found that loss of SRC-2 significantly enhanced the basal firing rate of POMC neurons without alterations in the resting membrane potential (Figures 1F–1H). The enhanced POMC firing activity may account for the impairments in energy expenditure suppression during fasting. Further, we found that the amplitude, but not the frequency, of the miniature inhibitory post-synaptic currents (mIPSCs) was significantly reduced in POMC neurons from pomcSRC-2-KO mice compared to controls (Figures 1I–1K). Consistently, the expression of multiple subunits of the $GABA_A$ receptor was significantly lower in POMC neurons lacking SRC-2 than in controls (Figure 1L). Thus, we suggest that SRC-2 maintains the responsiveness of POMC neurons to inhibitory GABAergic inputs via cell-autonomous regulations on the $GABA_A$ receptor expression.

SRC-2 in POMC neurons facilitates counterregulatory response

Consistent with previous reports (Claret et al., 2007; Parton et al., 2007; Santoro et al., 2017), we found that 57.69% of POMC neurons in control mice were glucose-excited (GE) neurons (excited by high glucose but inhibited by low glucose), while 21.15% of POMC neurons were glucose-inhibited (GI) neurons (inhibited by high glucose but excited by low glucose; Figures 2A and 2B). The percentage of GI-POMC neurons was not affected in pomcSRC-2-KO mice (pomcSRC-2-KO mice: 20.00% versus control: 21.15%; $p = 0.90$ in $\chi 2$ test), and their sensitivity (as demonstrated by changes in firing rate and resting membrane potential in response to low glucose) was not altered (Figures S2F and S2G). On the other hand, the percentage of GE-POMC neurons was significantly reduced in pomcSRC-2-KO mice (pomcSRC-2-KO mice: 37.14% versus control: 57.69%; $p < 0.05$ in $\chi 2$ test; Figures 2A and 2B). In other words, deletion of SRC-2 diminished the GE property of about 20% of POMC neurons. Even for those that remained to be GE-POMC neurons in pomcSRC-2-KO mice, their sensitivity was significantly reduced compared to GE-POMC

neurons in control mice (Figures 2C and 2D). ATP-sensitive potassium channel (K_{ATP}) has been reported to mediate the glucose-sensing function of POMC neurons (Parton et al., 2007; Santoro et al., 2017). Consistently, we found that, in control mice, pharmacological blockade of the K_{ATP} channel, by tolbutamide, abolished the glucose-sensing properties of GE-POMC neurons (Figures 2E and 2F). Further, we observed that lower glucose triggered robust K_{ATP} currents in GE-POMC neurons from control mice, but this effect was significantly blunted in GE-POMC neurons from pomcSRC-2-KO mice (Figures 2G and 2H). Consistently, the expression of all three subunits of the K_{ATP} channel was significantly reduced in GE-POMC neurons lacking SRC-2 (Figure 2I). These results indicate that SRC-2 is required to maintain the glucose-sensing properties of GE-POMC neurons via regulations on the expression of the K_{ATP} channel.

Impaired glucose-sensing properties of POMC neurons have been reported to cause whole-body glucose dysregulations (Claret et al., 2007; Parton et al., 2007; Santoro et al., 2017). Here, we found that administration of 2-DG (2-Deoxy-D-Glucose), which triggers glucopenia and mimics fasting, induced significant glucose elevations in control mice, but this effect was blunted in pomcSRC-2-KO mice (Figures 2J and 2K). We then performed hyperinsulinemic-hypoglycemic clamp in a cohort of body-weight-matched control and pomcSRC-2-KO littermates (Figure S2H). When blood glucose was clamped at 50 mg/dL, pomcSRC-2-KO mice required significantly higher glucose infusion to maintain this hypoglycemic level (Figures 2L and 2M), indicating an impaired counterregulatory response. Consistently, the plasma level of glucagon, a major counterregulatory hormone, was significantly lower in pomcSRC-2-KO mice than in controls (Figure 2N), although the corticosterone level was not significantly different (Figure S2I). On the other hand, pomcSRC-2-KO mice and controls showed similar glucose clearance in response to a glucose bolus challenge (Figure S2J). Thus, we suggest that SRC-2 in POMC neurons, although playing a minor role in hyperglycemic conditions, is essential for the counterregulatory response, a defensive mechanism to prevent severe hypoglycemia.

SRC-2 in POMC neurons promotes refeeding

Food intake of pomcSRC-2-KO mice, when fed chow *ad libitum*, was comparable to that of controls, and there was no alteration in the circadian pattern of feeding (Figures S2K–S2M). However, the 4-h refeeding (after a 24-h fasting) was significantly lower in pomcSRC-2-KO mice than in control mice (Figures 3A and S2N). Interestingly, after a 24-h fasting, control mice showed significantly enhanced maximal meal size and meal duration in the refeeding phase compared to the *ad libitum* feeding phase; on the other hand, these adaptations in feeding pattern were absent in pomcSRC-2-KO mice (Figures 3B and 3C). These results indicate that, although SRC-2 in POMC neurons plays a minor role in controlling food intake when fed *ad libitum*, it is required to enhance refeeding after food deprivation presumably by suppressing satiation.

Other important adaptations during refeeding include changes in mood that promote animals to search for food that is often associated with danger (Alhadeff et al., 2018; Burnett et al., 2016; Dietrich et al., 2015; Padilla et al., 2016; Wang et al., 2021). In particular, hunger can suppress anxiety, which facilitates animal's food-seeking behavior (Burnett et

al., 2016; Dietrich et al., 2015). In an elevated plus maze test (Figure 3D), mice avoid the open arms, which are associated with potential risks and therefore promote anxiety. Interestingly, we found that fasted control mice spent significantly more time in the open arms when chow pellets were present compared to empty open arms (Figures 3E–3G), indicating that hungry mice can overcome anxiety to pursue food. Strikingly, this behavioral adaptation was abolished in fasted pomcSRC-2-KO mice (Figures 3E–3G). Similarly, mice avoid the anxiogenic center region in the open-field test (Figure 3H). Although the presence of chow pellets in the center significantly increased time spent in the center by fasted control mice, this behavioral adaptation was abolished in fasted pomcSRC-2-KO mice (Figures 3I–3K). Importantly, fasted control and pomcSRC-2-KO mice showed comparable anxiety-like behaviors when there was no chow pellet available in the anxiogenic zones (Figures 3D–3K). These results indicate that SRC-2 in POMC neurons does not regulate anxiety per se but rather facilitates animal's mood adaptations to seek for food that is associated with potential danger.

SRC-2 coactivates FoxO1 transcriptional activity to regulate gene expression

In cultured cells, we found that SRC-2 strongly interacts with Forkhead box protein O1 (FoxO1) (Figure S3A). Given that FoxO1 directly suppresses POMC expression (Kitamura et al., 2006), we then tested whether SRC-2 regulates FoxO1's transcriptional activity on POMC expression. It is known that fasting triggers the translocation of FoxO1 from the cytosol to the nucleus (Fukuda et al., 2008; Kitamura et al., 2006; Plum et al., 2009). Thus, we first demonstrated that FoxO1 was primarily distributed in the cytosol of cells incubated in 10% serum (mimicking the "fed" condition), although incubation with 2% serum (stripped with charcoal) led to significant nuclear translocation of FoxO1 in these cells, which resembles the "fasted" condition (Figure S3B). Interestingly, using a POMC-luciferase assay, we found that fasted cells showed significantly lower POMC expression than fed cells, and overexpression of SRC-2 in fasted cells further decreased POMC expression (Figure 4A). Importantly, SRC-2 overexpression did not alter POMC expression in fed cells (Figure 4A), suggesting that nuclear FoxO1 is required for the suppressing effects of SRC-2 on POMC expression. Further supporting this notion, we showed that FoxO1 knockdown with small interfering RNA (siRNA) blocked the effects of SRC-2 on POMC expression in fasted cells (Figures 4B and S3C). Consistent with these *in vitro* observations, we detected the interaction between endogenous SRC-2 and FoxO1 in the mouse hypothalamus and further found that this interaction was significantly enhanced in fasted mice compared to mice fed *ad libitum* (Figure S3D). We then examined the effects of insulin, leptin, or cold exposure on this interaction between hypothalamic SRC-2 and FoxO1 but failed to detect significant changes (Figures S3E–S3G). Importantly, deletion of SRC-2 from POMC neurons significantly enhanced POMC expression in fasted mice (Figure 4C). Collectively, these results suggest that SRC-2 interacts with FoxO1 to facilitate its suppressing effects on POMC gene expression.

SRC-2 is known to interact with estrogen receptor α (ERα) and androgen receptors (ARs) to regulate gene expression (Dasgupta and O'Malley, 2014). Here, we found that overexpression of SRC-2 in 10% serum-incubated cells had no effect on POMC luciferase activity, either in the absence or in the presence of ERα/17β-estradiol (E2) or

AR/dihydrotestosterone (DHT), suggesting that SRC-2's interactions with ERα or with ARs do not influence POMC expression (Figures S4A and S4B). We also used luciferase assays to examine the effects of SRC-2 on the transcription of the $GABA_A$ receptor subunits and K_{ATP} channel subunits in cultured cells. We found that overexpression of SRC-2 significantly increased transcription of all these tested subunits (Figures S4C–S4K). Importantly, knockdown of FoxO1 attenuated SRC-2's transactivity on the majority of these subunits except for Kcnj8 (Figures S4C–S4K). Thus, our results suggest that the interactions between SRC-2 and FoxO1 regulate the expression of multiple genes.

SRC-2 in POMC neurons mediates FoxO1's orexigenic effects during overnutrition

We found that high fat-diet (HFD) feeding can enhance the hypothalamic SRC-2/FoxO1 interaction (Figure 4D). To examine the role of SRC-2 in HFD-induced obesity, we fed pomcSRC-2-KO mice and their control littermates with HFD *ad libitum*. During the 7-week HFD feeding, pomcSRC-2-KO mice gained significantly less body weight and fat mass compared to control mice (Figures 4E and 4F), associated with a significant decrease in HFD intake (Figure 4G). Given the known roles of FoxO1 in POMC neurons in mediating diet-induced obesity (Kitamura et al., 2006; Plum et al., 2009) and the functional interaction of SRC-2 and FoxO1, we postulated that SRC-2 coactivates FoxO1 in POMC neurons to promote body weight gain during HFD feeding. To test this, we constructed an AAV-FLEX-$FoxO1^{AAA}$-GFP virus, which expresses a constitutively active nuclear mutant $FoxO1^{AAA}$ (Thr24/Ser256/Ser319→alanine; (Tang et al., 1999) in a Cre-dependent manner (Figure S4L). Stereotaxic injections of this AAV vector into the ARH (both sides) of POMC-Cre mice resulted in overexpression of $FoxO1^{AAA}$ selectively in POMC neurons (Figure S4M). This $FoxO1^{AAA}$ overexpression caused significant increases in body weight gain, fat mass, and food intake in HFD-fed POMC-Cre mice, compared to wild-type (WT) littermates receiving the same AAV injections (Figures 4H–4K). Importantly, these $FoxO1^{AAA}$-induced obese and hyperphagic phenotypes were partially blunted in pomcSRC-2-KO mice (Figures 4H–4K), demonstrating that SRC-2 in POMC neurons facilitates orexigenic functions of FoxO1.

DISCUSSION

A series of coordinated responses are crucial for animals to survive periods of scarce food. When food is not available, animals need to suppress energy expenditure, which preserves energy storage; animals also need to promote counterregulatory responses in order to avoid severe hypoglycemia. Meanwhile, animals need to overcome anxiety and fear to seek for food that is often associated with danger (Alhadeff et al., 2018; Burnett et al., 2016; Dietrich et al., 2015; Padilla et al., 2016). Once the food is found, animals need to engage in efficient refeeding to prepare for the next potential fasting. Interestingly, we found that SRC-2 in POMC neurons is required for all these responses during the fasting-refeeding transition.

In response to food deprivation, mice lacking SRC-2 in POMC neurons are unable to effectively suppress energy expenditure. Importantly, the mutant mice lost more body weight and fat storage after food deprivation, indicating that the small deficits in suppressing energy expenditure in these mice are sufficient to result in significant damage to energy balance.

In addition, the loss of SRC-2 in POMC neurons also impairs counterregulatory responses and causes glucose dysregulations, especially during the hypoglycemic challenge. These deficits would render major disadvantages to animals' survival if they lived in a real wild environment with frequent periods of fasting. When food becomes available, these mutant mice show insufficient refeeding associated with enhanced satiation and discoordination of anxiety and food-seeking behavior. Interestingly, all these deficits are not apparent when mice are fed *ad libitum*. Thus, SRC-2 is an essential gene to help animals survive the scarcity of food.

As a transcriptional co-activator, SRC-2 functions primarily through regulations on gene expression. One key gene in POMC neurons that is regulated by SRC-2 is the POMC gene itself. We observed increased POMC mRNA levels in mice lacking SRC-2 in POMC neurons. Consistently, SRC-2 overexpression can inhibit POMC transcription in cultured cells. In addition, we provided several pieces of evidence to suggest that SRC-2 regulates POMC gene expression through coactivating FoxO1's suppressing effects on the POMC promoter. First, we showed that SRC-2 and FoxO1 form a protein-protein complex in cells and in the mouse hypothalamus. Second, SRC-2 can suppress POMC expression only in fasted cells where FoxO1 exists in the nucleus, but these effects are not present in fed cells with FoxO1 primarily localized in the cytosol. Further, SRC-2's inhibitory effects on POMC expression are abolished by FoxO1 knockdown. Importantly, we showed that POMC-specific overexpression of a constitutively active nuclear mutant $FoxO1^{AAA}$ increases body weight and food intake in mice, but these responses are blunted in mice lacking SRC-2 in POMC neurons. Together, these observations support a model that SRC-2 coactivates the suppressing effects of FoxO1 on POMC expression. Notably, loss of FoxO1 in POMC neurons results in similar impairment in fasting-induced refeeding (Plum et al., 2009), as we observed in mice lacking SRC-2 in POMC neurons, further highlighting an important role of SRC-2/FoxO1 signaling in physiological responses during the fasting-refeeding transition. However, POMC-specific deletion of FoxO1 also decreases food intake and body weight when mice are fed chow *ad libitum* (Plum et al., 2009), phenotypes that are not recapitulated by SRC-2 deficiency. Thus, we suggest that, although SRC-2 is required for a portion of FoxO1 functions, FoxO1 likely also recruits other coactivators for other functions.

We also observed that loss of SRC-2 decreases the expression of multiple subunits of the $GABA_A$ receptor in POMC neurons. Consistently, POMC neurons in mutant mice show decreased mIPSC amplitude, associated with increased basal firing rate. In addition, glucose-sensing properties of GE-POMC neurons are impaired in mutant mice, presumably due to reduced expression of the K_{ATP} subunits. Thus, we suggest that SRC-2 regulates basal activity of POMC neurons and their response to glucose fluctuations through influencing the expression of the $GABA_A$ receptor and K_{ATP} subunits. Notably, the glucose-sensing properties of GI-POMC neurons are not affected by SRC-2 deletion, suggesting that different ionic mechanisms likely exist in GI neurons to regulate their responses to glucose fluctuations (He et al., 2020; Levin et al., 1999), which are not influenced by SRC-2 transcriptional coactivity. Interestingly, our data indicate that SRC-2 stimulates the expression of many of these $GABA_A$ receptor and K_{ATP} channel subunits in a FoxO1-dependent manner. The expression of one K_{ATP} subunit, Kcnj8, can be enhanced by

SRC-2 via a FoxO1-independent mechanism, suggesting that SRC-2 may coactivate other transcription factors for such an effect.

It is interesting to note that SRC-2 in other metabolic tissues has been shown to facilitate various adaptive responses to counteract food deprivation. For example, during fasting-induced refeeding, SRC-2 in the liver increases bile acid secretion in the gut; this SRC-2-mediated bile acid secretion is essential to promote energy intake through increasing fat absorption from the gut without increasing feeding per se (Chopra et al., 2011). Hepatic SRC-2 is also shown to promote gluconeogenesis during food deprivation (Chopra et al., 2008), which also contributes to the prevention of severe hypoglycemia. Further, SRC-2 in brown adipose tissue inhibits functions of PPARγ (peroxisome proliferator-activated receptor) and PGC1α (PPAR gamma coactivator 1) and therefore suppresses thermogenesis and energy expenditure (Picard et al., 2002). Similarly, SRC-2 in the muscle functions to suppress energy expenditure via inhibiting mitochondrial uncoupling in muscle cells (Duteil et al., 2010). These observations from the peripheral tissues, together with our findings in the hypothalamus, support a model where SRC-2 in various tissues functions synergistically, although via different biological processes and molecular mechanisms, to inhibit energy expenditure and to promote energy intake and ultimately ensures survival during periods of food scarcity. Although many genes are essential for survival during food shortage over evolutionary time (Neel, 1999), their energy-preserving functions may become detrimental in the face of excess nutrition that is more common in the modern environment. Supporting this notion, we found that mice lacking SRC-2 in POMC neurons mice were partially protected from HFD-induced obesity, associated with decreased HFD intake.

In summary, we showed that SRC-2 in POMC neurons is the key regulator of many metabolic and neurobehavioral adaptations essential for animals to survive food deprivation. These include suppression of energy expenditure and promotion of counterregulatory responses during fasting. When food becomes available, SRC-2 suppresses satiation and anxiety, allowing animals to refeed efficiently. Interestingly, these SRC-2 functions become detrimental in mice challenged with an obesogenic diet and promote obesity development. At the mechanistic level, we showed that SRC-2 controls the excitability of POMC neurons and their electric responses to glucose fluctuations. Further, SRC-2 coactivates FoxO1 to regulate the expression of multiple genes. Collectively, our results identified hypothalamic SRC-2 as a key molecule that coordinates multifaceted adaptive responses to food shortage and promotes body weight gain in the context of overnutrition.

Limitations of the study

SRC-2 is known to coactivate receptors of gonadal hormones, including ERα and ARs (Dasgupta and O'Malley, 2014). Indeed, we observed a robust co-localization of SRC-2 and ERα in the ARH and VMH. However, we failed to observe a functional interaction of SRC-2 and ERα or ARs to regulate POMC gene expression in an *in vitro* assay. In addition, most of the animal experiments were conducted in male mice only. Thus, our results could not exclude the possibility that SRC-2 proteins, e.g., those co-expressed by ERα neurons in the ARH and VMH, may influence signaling of gonadal hormones to regulate energy balance (Xu and López, 2018; Xu et al., 2011). Another limitation of the

study is the incomplete deletion of SRC-2 in a small portion of POMC neurons, which may have confounded the phenotypic outcome in pomcSRC-2-KO mice. In addition, because POMC-Cre induces DNA recombination during early development (Padilla et al., 2012), we could not exclude the potential contributions of altered POMC neuron development to the phenotypes we observed in these mutant mice.

STAR★METHODS

RESOURCE AVAILABILITY

Lead contact—Dr. Yong Xu (yongx@bcm.edu) is the lead contact of this work.

Materials availability—Animal models and viral vectors generated in this work will be made available upon request under MTAs.

Data and code availability—All data reported in this paper will be shared by the lead contact upon request. This paper does not report original code. Any additional information required to reanalyze the data reported in this paper is available from the lead contact upon request.

EXPERIMENTAL MODEL AND SUBJECT DETAILS

We crossed POMC-Cre transgenic mice (Balthasar et al., 2004) and SRC-$2^{lox/lox}$ mice (Picard et al., 2002). This cross produced pomcSRC-2-KO mice (those that are homozygous for SRC-$2^{lox/lox}$ and also carry the POMC-Cre transgene) and control mice (those that are homozygous for SRC-$2^{lox/lox}$ but do not carry the POMC-Cre transgene). These littermates were used to characterize the metabolic profile. For histology validation, electrophysiological recordings, and single neuron qRT-PCR, we crossed the POMC-eGFP mouse allele (Parton et al., 2007) onto pomcSRC-2-KO and control mice to label mature POMC neurons with GFP. In addition, we crossed the Rosa26-LSL-tdTOMATO mouse allele (Madisen et al., 2010) onto POMC-Cre (control) and pomc-SRC-2-KO mice to label all POMC-lineage neurons for histology validation. Further, we crossed the Rosa26-LSL-tdTOMATO mouse allele onto AgRP-IRES-Cre (Tong et al., 2008) to label AgRP neurons for histology; ERα-Zs-Green mice (Saito et al., 2016) were also used to label ERα-expressing neurons. Mice were housed in a temperature-controlled environment in groups of two to five at 22°C-24°C using a 12 hr light/12 hr dark cycle. The mice were fed standard chow (6.5% fat, #2920, Harlan-Teklad, Madison, WI) or a high fat-diet (HFD, 60% fat, #D12492, Research Diets). Water was provided *ad libitum*.

METHOD DETAILS

Histological analysis of SRC-2 expression in hypothalamic neurons—To examine the expression of SRC-2 in AgRP and ERα neurons, AgRP-IRES-Cre/Rosa26-LSL-tdTOMATO mice and ERα-ZsGreen mice were transcardially perfused with saline, followed by 10% formalin. The brain sections were cut at 25 μm and collected into five consecutive series. One series of the sections were blocked with 3% normal donkey serum for 1.5 hours, incubated with rabbit anti-SRC-2 antibody (1:1,000; #ab10491, Abcam, Boston, MA) on shaker at 4°C for overnight, followed by the donkey anti-rabbit AlexaFluor

488 (1:500; #A21206, Invitrogen, Grand Island, NY) or donkey anti-rabbit AlexaFluor 594 (1:500; #A21207, Invitrogen, Grand Island, NY) for 2 hours. Slides were coverslipped and analyzed using a Leica 5500 OptiGrid fluorescence microscope. To check the co-expression of SRC-2 and TH in the ARH, wild-type mice were perfused and sectioned. The brain sections were blocked with 3% normal goat serum for 1.5 hours, then incubated with rabbit anti-SRC-2 antibody (1:1,000; #ab10491, Abcam, Boston, MA) and chicken anti-TH antibody (1:2,000; #ab76442, Abcam, Boston, MA) on shaker at 4°C for overnight, followed by the donkey anti-rabbit AlexaFluor 488 (1:500; #A21206, Invitrogen, Grand Island, NY) and goat anti-chicken AlexaFluor 594 (1:500; #A11042, Invitrogen, Grand Island, NY) for 2 hours. Slides were coverslipped and analyzed using the Leica 5500 OptiGrid fluorescence microscope.

Validation of SRC-2 deletion in mature POMC neurons—POMC-eGFP mice and pomcSRC-2-KO/POMC-eGFP mice were perfused at 9 weeks of age, and therefore GFP-labeled neurons were identified as mature POMC neurons at this age. Brain sections were cut at 25 μm (1:5 series) and subjected to dual immunofluorescent staining for GFP and SRC-2. Briefly, the sections were incubated in the primary rabbit anti-SRC-2 antibody (1:1000; #A300–345A, Bethyl Laboratories, Inc., Montgomery, TX) overnight, followed by donkey anti-rabbit Alexa Fluor 594 (1:500; #A21207, Invitrogen, Grand Island, NY) for 1.5 hr. Then, the sections were incubated in primary chicken anti-GFP antibody (1:5000; #GFP-1020, Aves Labs, Inc., Tigard, OR) overnight, followed by the goat anti-chicken Alexa Fluor 488 (1:500; #A11039, Invitrogen, Grand Island, NY) for 1.5 hr. Slides were coverslipped and analyzed using the Leica 5500 OptiGrid fluorescence microscope. As shown in Figure 1A, while SRC-2 was co-expressed by the majority of GFP-labeled neurons in control mice, it was absent in these mature POMC neurons in pomcSRC-2-KO mice.

Since POMC-Cre may also cause DNA recombination in broad populations of neurons during early development (Padilla et al., 2010, 2012), we compared the expression of SRC-2 in tdTOMATO-labeled POMC-lineage neurons in POMC-Cre/Rosa26-LSL-tdTOMATO (control) and pomc-SRC-2-KO/Rosa26-LSL-tdTOMATO mice. Similarly, these mice (9 weeks of age) were perfused and fixed brains were cut at 25 μm (1:5 series). Brain sections were incubated in the primary rabbit anti-SRC-2 antibody (1:1000; #A300–345A, Bethyl Laboratories, Inc.) overnight, followed by donkey anti-rabbit Alexa Fluor 488 (1:500; #A21207, Invitrogen) for 1.5 hr; red tdTOMATO fluorescent signals were directly visualized without any immunostaining process. As shown in Figures S1A and S1B, while POMC-Cre-induced tdTOMATO expression in the medial subdivision of the ARH (presumably AgRP/NPY neurons) and in the hippocampal DG region, SRC-2 was not deleted in these POMC-lineage neurons in pomcSRC-2-KO mice. Consistent with the previous report (Padilla et al., 2012), scattered TOMATO-labeled POMC-lineage neurons were also observed in the septal nucleus, the preoptic area, the amygdala, the central thalamus, the interpeduncular fossa, the periaqueductal gray, the area postrema, the nucleus of solitary tract and the cochlear nucleus, but SRC-2 was not deleted in these neurons in pomcSRC-2-KO mice (data not shown but available upon request).

Characterization of energy homeostasis—pomcSRC-2-KO mice and their control littermates were weaned at week 4 on the standard chow (6.5% fat, #2920, Harlan-Teklad) and singly housed. Some mice were switched to the HFD (60% fat, #D12492, Research Diets) from 7 weeks of age. Body weight and food intake were measured weekly. Body composition was determined using quantitative magnetic resonance (QMR). At the end of monitoring, the mice were deeply anesthetized with inhaled isoflurane and sacrificed, and the gonadal white adipose tissue, the inguinal white adipose tissue, and the interscapular brown adipose tissue were isolated and weighed.

To characterize the responses to food deprivation, some mice (4 months of age) were subjected to a 24-hour fasting, and body weight and body composition were measured before and after the fasting. Fasting-induced refeeding was assessed in a cohort of mice after a 24-hour fasting in their home cages. To further characterize the food intake and energy expenditure, another male cohort (pomcSRC-2-KO mice and their control littermates, 3 months of age) were acclimated into the Comprehensive Laboratory Animal Monitoring System (CLAMS). Mice were housed individually at room temperature (22°C) under an alternating 12:12-h light-dark cycle. After adaptation for 3 days, mice were subjected to a 3-day protocol with 24-hour (6 am-6 am) feed *ad libitum*, 24-hour fast and 24-hour refeed. O_2 consumption, CO_2 production and energy expenditure were monitored; meal size and meal duration were analyzed with the CLAMS system. Note that, the body weight and body composition were measured before the mice entered the CLAMS cages, and no difference was observed in body weight, fat mass, and lean mass.

Anxiety tests with or without food—Fasted control and pomcSRC-2-KO mice (male, 3–4 months of age) were subjected to the open field tests and the elevated plus maze tests, similarly as we did before (Xu et al., 2015). Note that all the behavioral tests were performed at around 1–4 pm during the light cycles. Briefly, the open-field test was performed in a clear Plexiglas open-field arena (40 cm X 40 cm X30 cm). Mice, after a 20-hour fasting, were placed into the center of the arena and allowed to explore for 30 min. Overhead lighting and white noise were present to provide ~800 lux illumination and ~55 dB sound inside the arena. Data were collected in 2 min intervals by a computer-operated Digiscan optical animal activity system (RXYZCM, Accuscan Electronics). For the current study, the data over the total 30-min test session were analyzed. Center time (the time traveled in the center of the arena) were recorded. The same experiments were repeated in fasted mice with chow pellets placed in the center of the arena.

On a different day, these mice were subjected to the elevated plus maze (EPM). The EPM was constructed of Plexiglas with two open arms (30 × 5 cm) and two enclosed arms (30 × 5 × 15 cm) at an elevation of 50 cm above the floor. The arms of the maze form a cross with the two open arms facing each other. The maze was cleaned with 70% ethanol solution after each session and allowed to dry between the sessions. The mice were placed in the center of the junction of the arms of the maze facing an open arm and the behavior was analyzed for 10 min. The time spent exploring the open and closed arms was recorded and analyzed using the ANY-maze software (Stoelting Co., Wood Dale, IL). The same experiments were repeated in fasted mice with chow pellets placed in the open arms.

Electrophysiology—POMC-eGFP or pomcSRC-2-KO/POMC-eGFP mice were used for electrophysiological recordings. Mice were deeply anesthetized with isoflurane and transcardially perfused with a modified ice-cold sucrose-based cutting solution (pH 7.3) containing 10 mM NaCl, 25 mM NaHCO3, 195 mM Sucrose, 10 mM Glucose, 2.5 mM KCl, 1.25 mM NaH2PO4, 2 mM Na-Pyruvate, 0.5 mM CaCl2, and 7 mM MgCl2, bubbled continuously with 95% O2 and 5% CO2. The mice were then decapitated, and the entire brain was removed and immediately submerged in the cutting solution. Slices (250 μm) were cut with a Microm HM 650V vibratome (Thermo Scientific). Three brain slices containing the ARH were obtained for each animal (Bregma −2.06 mm to −1.46 mm). The slices were recovered for 1 h at 34°C and then maintained in artificial cerebrospinal fluid (aCSF, pH 7.3) containing 126 mM NaCl, 2.5 mM KCl, 2.4 mM CaCl2, 1.2 mM NaH2PO4, 1.2 mM MgCl2, 5.0 mM glucose, and 21.4 mM NaHCO3) saturated with 95% O2 and 5% CO2 before recording.

Slices were transferred to a recording chamber and allowed to equilibrate for at least 10 min before recording. The slices were superfused at 34°C in oxygenated aCSF at a flow rate of 1.8–2 ml/min. GFP-labeled mature POMC neurons in the ARH were visualized using epifluorescence and IR-DIC imaging on an upright microscope (Eclipse FN-1, Nikon) equipped with a movable stage (MP-285, Sutter Instrument). Patch pipettes with resistances of 3–5 MΩ were filled with intracellular solution (pH 7.3) containing 128 mM K-Gluconate, 10 mM KCl, 10 mM HEPES, 0.1 mM EGTA, 2 mM MgCl2, 0.05 mM $(Na)_2$GTP and 0.05 mM (Mg)ATP. Recordings were made using a MultiClamp 700B amplifier (Axon Instrument), sampled using Digidata 1440A and analyzed offline with pClamp 10.3 software (Axon Instruments). Series resistance was monitored during the recording, and the values were generally < 10 MΩ and were not compensated. The liquid junction potential was +12.5 mV, and was corrected after the experiment. Data were excluded if the series resistance increased dramatically during the experiment or without overshoot for action potential. Currents were amplified, filtered at 1 kHz, and digitized at 20 kHz. In order to examine the glucose-sensing functions, neurons were recorded under the current clamp mode in response to a 5→1→5 mM extracellular glucose fluctuation protocol (He et al., 2020; Kong et al., 2010; Yu et al., 2020). The values for resting membrane potential and firing rate were averaged within 2-min bin at the 5 mM glucose or 1 mM glucose aCSF condition. A neuron was considered depolarized or hyperpolarized if a change in membrane potential was at least 2 mV in amplitude. Tolbutamide (100 μM, a K_{ATP} blocker) (Kong et al., 2010) was added in some experiments to determine if it can block or attenuate changes in firing rate and resting membrane potential induced by glucose fluctuations.

To directly record K_{ATP} currents, slices were perfused with an external solution that contained 140 mM NaCl, 5 mM KCl, 2 mM CaCl2, 1 mM MgCl2, 5 mM glucose and 10 mM HEPES (pH 7.4). The pipette (intracellular) solution contained 130 mM potassium gluconate, 20 mM HEPES, 10 mM EGTA, 1 mM MgCl2, 2.5 mM CaCl2, 1.0 mM Mg-ATP, and 0.3 mM Tris-GTP (pH 7.2) (Grabauskas et al., 2015). The neural membrane potential was held at −60 mV in voltage clamp model when K_{ATP} current was recorded when glucose was changed from 5 mM to 1 mM. Tolbutamide (100 μM) was added in some experiments to determine if it can block or attenuate the currents. Miniature inhibitory post-

synaptic currents (mIPSCs) were recorded in whole-cell voltage-clamp mode, by holding the membrane potential at Vh = −70 mV in the presence of 1 μM TTX, 30 μM CNQX and 30 μM D-AP5. The CsCl-based pipette solution containing of: 140mM CsCl, 10mM HEPES, 5mM $MgCl_2$, 1mM BAPTA, 5mM (Mg)ATP, and 0.3mM $(Na)_2GTP$ (pH 7.30 adjusted with NaOH; 295 mOsm kg^{-1}). After the recording of each neuron, an Alexa Fluor 594 dye was injected into the recorded neuron via the pipette. Slices were fixed with 4% formalin in PBS at 4°C overnight and then subjected to post hoc identification of the anatomical location of the recorded neurons within the ARH.

qRT-PCR—To examine gene expression specifically in POMC neurons, we manually picked up GFP-labeled neurons from POMC-eGFP or pomcSRC-2-KO/POMC-eGFP mice. To this end, the mice brain was removed and immediately submerged in ice-cold sucrose-based cutting solution (adjusted to pH 7.3) containing (in mM) 10 NaCl, 25 NaHCO3, 195 Sucrose, 5 Glucose, 2.5 KCl, 1.25 NaH2PO4, 2 Na pyruvate, 0.5 CaCl2, 7 MgCl2 bubbled continuously with 95% O2 and 5% CO2. The slices (250 μm) were cut with a Microm HM 650V vibratome (Thermo Scientific and recovered for 1 h at 34°C and then maintained at room temperature in artificial cerebrospinal fluid (aCSF, pH 7.3) containing 126 mM NaCl, 2.5 mM KCl, 2.4 mM CaCl2, 1.2 mM NaH2PO4, 1.2 mM MgCl2, 11.1 mM glucose, and 21.4 mM NaHCO3 saturated with 95% O2 and 5% CO2 before recording. Slices were transferred to a chamber, and GFP-labeled neurons were visualized using epifluorescence and IR-DIC imaging on an upright microscope equipped with a moveable stage (MP-285, Sutter Instrument). In some experiments, these neurons were first subjected to electrophysiological recordings to determine whether they were GE neurons or not, as described above. Single GE neurons were then manually picked up by the pipette and 2 neurons were combined as a sample for RNA extraction and reverse transcription using the Ambion Single-Cell-to-CT Kit (Ambion, Life Technologies) according to the manufacturer's instruction. Briefly, 10 μL Single Cell Lysis solutions with DNase I was added to each sample, and the supernatant after centrifuge were used for cDNA synthesis (25°C for 10 min, 42°C for 60 min, and 85°C for 5 min). The cDNA samples were amplified on a CFX384 Real-Time System (Bio-Rad) using SsoADV SYBR Green Supermix (Bio-Rad). Results were normalized against the expression of the house-keeping gene (b-actin). Primer sequences were listed in Table S1.

In some experiments, fasted control and pomcSRC-2-KO mice (male, 4–5 months of age) were sacrificed and the hypothalami were quickly collected. Total RNA was isolated using TRIzol Reagent (Invitrogen) according to the manufacturer's protocol and reverse transcription reactions were performed from 2 μg of total RNA using a High-Capacity cDNA Reverse Transcription Kits (Invitrogen). cDNA samples were amplified on an CFX384 Real-Time System (Bio-Rad) using SsoADV SYBR Green Supermix (Bio-Rad). Results were normalized against the expression of house-keeping gene (cyclophinlin). Primer sequences were listed in Table S1.

Glucose tolerance test and 2-DG assay—Control and pomcSRC-2-KO mice (male, 3–4 months of age) received i.p. injections of glucose (1 g/kg). Blood glucose was then measured at 0, 15, 30, 60 and 120 min after injections. Similarly, control and pomcSRC-2-

KO mice (male, 3–4 months of age) received i.p. injections of saline or 2-DG (500 mg/kg). Blood glucose was then measured at 0, 15, 30, 60 and 120 min after injections.

Hyperinsulinemic-hypoglycemia clamp—Body weight-matched control and pomcSRC-2-KO mice (male, 3–4 months of age) were sent to the NIH-funded Baylor Mouse Metabolism Core for the hyperinsulinemic-hypoglycemic clamp studies. As we described before (Zhu et al., 2015), a micro-catheter was inserted into the jugular vein by survival surgery and waited for 4–5 days for complete recovery. Studies were then performed in conscious mice. Overnight-fasted conscious mice received a priming dose of HPLC-purified [3–3H] glucose (10μCi) and then a constant infusion (0.1 μCi/min) of label glucose for ~2.5–3.0 hr. After ~1h of infusion, mice were primed with regular insulin (bolus 10 mU/kg body weight) followed by a ~2-hr constant insulin infusion (10 mU/Kg/min). Using a separate pump, 25% glucose was used to maintain the blood glucose level at 50 mg/dl, as determined every 6–9 min using a glucometer (LifeScan, NJ). The glucose infusion rate (GIR) was then measured. Blood samples were collected during the hypoglycemic condition and processed to obtain plasma. These samples were sent to the VUMC (Vanderbilt University Medical Center) Hormone Assay & Analytical Services Core to measure glucagon; corticosterone was measured using Corticosterone ELISA kit (Enzo Life Sciences) according to the manufacturer's instructions.

Overexpression of FoxO1^{AAA} in POMC neurons—AAV-FLEX-FoxO1^{AAA}-GFP was constructed by sub-cloning the full length of Foxo1^{AAA} (Tang et al., 1999) into the pAAV-hSyn1-FLEX-2A-GFP vector (Wang et al., 2018). Virus was packaged at Neuroconnectivity Core at Jan and Dan Duncan Neurological Research Institute with serotype AAV2/8. WT, POMC-Cre and pomcSRC-2-KO mice (male, 4–5 months of age) were anesthetized with isoflurane and received stereotaxic injections of AAV-FLEX-FoxO1^{AAA}-GFP into both sides of the ARH (250 nL/site, −1.7 mm posterior, ± 0.25 mm lateral and −5.8 mm ventral to the Bregma, based on Franklin & Paxinos Mouse Brain Atlas). In addition, another group of pomcSRC-2-KO mice (male, 4–5 months of age) received AAV-GFP injections into the ARH. One week after the virus injections, mice were fed on HFD for 3 weeks. Body weight and food intake were monitored weekly. Body weight composition was measured at the end of HFD feeding. To validate accurate and sufficient infection of AAV vectors, all mice were perfused with 10% formalin. Brain sections were cut at 25 μm (5 series) and subjected to histological validation. Only those mice with GFP in both sides of the ARH were included in data analyses.

SRC-2 and FoxO1 interaction—For *in vitro* SRC-2 and FoxO1 interaction, HEK293 (Human embryonic kidney 293) cells were transfected with Flag-tagged FoxO1 or empty vector using lipofectamine 2000 (Invitrogen). Two days after transfection, cells were lysed with cell lysis buffer: 50 mM Tris, 50 mM KCL, 10 mM EDTA, 1% NP-40, supplied with protease inhibitor cocktail (Roche) and phosphatase inhibitor cocktail A (Santa Cruz). The lysates were incubated with a proper amount of anti-Flag-beads (Sigma) for 4 h at 4°C. Beads were washed three times with lysis buffer, and proteins were released from beads in SDS-sample buffer and analyzed by immunoblotting. The blot was probed with anti-Flag-HRP (1:3,000–10,000, A8592, Sigma), rabbit polyclonal

anti-SRC-2 antibody (1:1,000, ab10491, Abcam) or mouse monoclonal anti-β-Actin-HRP (1:5,000, #12262, Cell Signaling), and the secondary antibody was goat anti-rabbit IgG (Jackson ImmunoResearch), followed by development with the SuperSignal West Pico Chemiluminescent Substrate (Pierce).

In vivo interaction between SRC-2 and FoxO1 was investigated under different conditions. For fed and fasted conditions, C57Bl6j male mice (3 months of age) were sacrificed at fed condition or after a 24-hour fasting. For Insulin or Leptin treatment, C57Bl6j fed male mice were i.p. injected with saline, insulin (3U/kg) or leptin (5 mg/kg), and the hypothalami were collected 30 min after the injections. For cold exposure, singly caged C57Bl6j fed male mice were kept at 4°C or room temperature (RT) for 6 hours before the hypothalami were collected. For chow and HFD feeding conditions, C57Bl6j male mice (3 months of age) were fed on regular chow or the HFD for 2 weeks *ad libitum*, and then sacrificed at fed condition. Harvested hypothalami were lysed in lysis buffer (50 mM Tris-HCl, pH 8.0, 50 mM KCl, 20 mM NaF, 1 mM Na3VO4, 10 mM sodium pyrophosphate, 5 mM EDTA, and 0.5% Nonidet P-40) supplemented with protease inhibitor cocktail (Roche) and phosphatase inhibitor cocktail A (Santa Cruz). Lysates were cleared by centrifugation at 18,000 × *g* for 10 min and used for immunoprecipitation or directly for immunoblotting. Equal amounts of tissue lysates were incubated with rabbit monoclonal anti-FoxO1 (1:100, #2880, Cell Signaling) for 1 hr. at 4°C and pulled down with Protein G magnetic beads (70024, Cell Signaling). The proteins were analyzed by immunoblotting with rabbit monoclonal anti-FoxO1 antibody (1:3,000, #2880, Cell Signaling) or mouse monoclonal anti-FoxO1 antibody (1:3,000, #97635, Cell Signaling), rabbit polyclonal anti-SRC-2 antibody (1:1,000, ab10491, Abcam) or mouse monoclonal anti-β-Actin-HRP (1:5,000, #12262, Cell Signaling), and the secondary antibody was rabbit anti-mouse IgG or goat anti-rabbit IgG (Jackson ImmunoResearch), followed by development with the SuperSignal West Pico Chemiluminescent Substrate (Pierce).

POMC-luciferase assay—For the POMC-luciferase assay, an embryonic mouse hypothalamic cell line, N46 (CELLutions), was cultured in Dulbecco's modified Eagle's medium supplemented with 10% fetal bovine serum (Atlanta), 100 IU/ml penicillin and 100 ng/ml streptomycin. To verify the FoxO1 intracellular localization under different nutritional conditions, N46 cells were cultured in full media (containing 10% FBS) or "fast" media (2% charcoal-stripped FBS) for overnight. The FoxO1 was stained with anti-FoxO1 (#2880, Cell Signaling) and combined with Donkey anti-Rabbit IgG Alexa Fluor 594 (A21207, Thermo fisher scientific). To measure SRC-2 activity on the POMC promoter, N46 cells were seeded into a 24-well plate overnight and then transfected with 500 ng of the POMC-luciferase reporter plasmid combined with 100 ng of pCR3.1-SRC-2 or the control empty plasmids, according to the Lipofectamine LTX protocol (Invitrogen). Twenty four hours after the transfection, the cells were switched to full media culture (containing 10% FBS) or "fast" media (2% charcoal-stripped FBS) for overnight. The luciferase activity was measured using the Luciferase Reporter Assay System (Promega) according to the manufacturer's instructions. To further investigate the effect of SRC-2/FoxO1 interaction on the POMC promoter activity, FoxO1 siRNA (mouse-specific #6468, Cell Signaling) or control siRNA (#6568, Cell Signaling) was transfected into the N46 cells using Lipofectamine RNAiMAX

(Invitrogen). Twenty four hours after the transfection, the cells were further transfected with 500 ng of the POMC-luciferase reporter plasmid combined with 100 ng of pCR3.1-SRC-2 or the empty control plasmids using Lipofectamine LTX. Twenty four hours after the transfection, cells were switched to “fast” media (2% charcoal-stripped FBS) for overnight culture and then the luciferase activity was measured using the Luciferase Reporter Assay System. The FoxO1 siRNA knockdown effects were confirmed by immunoblotting 2 days after the transfection of the FoxO1 siRNA or the control siRNA, with monoclonal anti-FoxO1 (1:3,000, #2880, Cell Signaling) and anti-Actin antibody (#C-11, Santa Cruz).

To test the effects of the interaction between SRC-2 and ERα or AR on the regulation of POMC expression, POMC-luciferase reporter was co-transfected with pCR3.1-SRC-2 or the empty control plasmids, with or without pcDNA3.1-hERα (Yang et al., 2019) or pCMV-FLAG-hAR (a gift from Elizabeth Wilson, Addgene plasmid # 89080) (Bai et al., 2005) as described above. Forty hours after the transfection, cells were treated with or without 17β-estradiol (0.2 μg/ml, E-060, Sigma) or DHT (10 nM, D-073, Sigma) for 8 hours, and then the luciferase activity was measured using the Luciferase Reporter Assay System.

To further test how SRC-2 regulates the expression of $GABA_A$ receptor subunits and K_{ATP} channel subunits, the promoter region of each gene was cloned into pGL3-basic Luciferase Reporter Vector (primer sequences shown in Table S2), and each luciferase reporter was co-transfected with pCR3.1-SRC-2 or the empty control plasmids for two days. To further investigate the effect of SRC-2/FoxO1 interaction on these promoters activity, similar method was used for the FoxO1 knockdown and the luciferase assay was performed as described above.

QUANTIFICATION AND STATISTICAL ANALYSIS

The minimal sample size was pre-determined by the nature of experiments. For most of the physiological readouts (body weight, food intake, etc.), at least 6 mice per group were included. For electrophysiological studies, at least 8 neurons per group were included. The data are presented as mean ± SEM. Statistical analyses were performed using GraphPad Prism to evaluate normal distribution and variations within and among groups. Methods of statistical analyses were chosen based on the design of each experiment and are indicated in figure legends. $p < 0.05$ was considered to be statistically significant.

Study approval—Care of all animals and procedures were approved by the Baylor College of Medicine Institutional Animal Care and Use Committee.

Supplementary Material

Refer to Web version on PubMed Central for supplementary material.

ACKNOWLEDGMENTS

The investigators were supported by grants from the NIH (R01DK114279, R01DK109934, and R21NS108091 to Q.T.; R00DK107008 to P.X.; R01DK104901 and R01DK126655 to M.F.; K01DK119471 to C.W.; R01DK115761, R01DK117281, and R01DK125480 to Y.X.; R01DK120858 to Q.T. and Y.X.; R01DK111436, R01ES027544,

RF1AG069966, HL153320, and AG070687 to Z.S.; R01HD07857, R01HD008818, and P01DK059820 to B.W.O.; P01DK113954 to Y.X., J.X., and B.W.O.; and P20 GM135002 to Y.H.), USDA/CRIS (51000-064-01S to Y.X. and M.F.), American Diabetes Association (1-17-PDF-138 to Y.H.), and American Heart Association awards (16POST27260254 to C.W.). Measurements of body composition, food intake, and energy expenditure were performed in the Mouse Metabolic Research Unit (MMRU) at the USDA/ARS Children's Nutrition Research Center, Baylor College of Medicine, which is supported by funds from the USDA ARS (https://www.bcm.edu/cnrc/mmru). The *SRC-2*$^{lox/lox}$ mouse line was provided by Dr. Pierre Chambon (IGBMC/GIE-CERBM). The authors acknowledge the expert assistance of Mr. Firoz Vohra and the MMRU Core Director, Dr. Marta Fiorotto. The open-field test and elevated plus maze test were performed in the Mouse Neurobehavior Core, Baylor College of Medicine, which is supported by NIH P30HD024064. The AAV vector expressing FoxO1^{AAA} mutant was packaged by Baylor IDDRC Neuroconnectivity Core directed by Dr. Benjamin Arenkiel.

REFERENCES

Ahima RS, Prabakaran D, Mantzoros C, Qu D, Lowell B, Maratos-Flier E, and Flier JS (1996). Role of leptin in the neuroendocrine response to fasting. Nature 382, 250–252. [PubMed: 8717038]

Ahima RS, Kelly J, Elmquist JK, and Flier JS (1999). Distinct physiologic and neuronal responses to decreased leptin and mild hyperleptinemia. Endocrinology 140, 4923–4931. [PubMed: 10537115]

Alhadeff AL, Su Z, Hernandez E, Klima ML, Phillips SZ, Holland RA, Guo C, Hantman AW, De Jonghe BC, and Betley JN (2018). A Neural Circuit for the Suppression of Pain by a Competing Need State. Cell 173, 140–152 e115. [PubMed: 29570993]

Bai S, He B, and Wilson EM (2005). Melanoma antigen gene protein MAGE-11 regulates androgen receptor function by modulating the interdomain interaction. Mol. Cell. Biol. 25, 1238–1257. [PubMed: 15684378]

Balthasar N, Coppari R, McMinn J, Liu SM, Lee CE, Tang V, Kenny CD, McGovern RA, Chua SC Jr., Elmquist JK, and Lowell BB (2004). Leptin receptor signaling in POMC neurons is required for normal body weight homeostasis. Neuron 42, 983–991. [PubMed: 15207242]

Burnett CJ, Li C, Webber E, Tsaousidou E, Xue SY, Bruning JC, and Krashes MJ (2016). Hunger-Driven Motivational State Competition. Neuron 92, 187–201. [PubMed: 27693254]

Caron A, Dungan Lemko HM, Castorena CM, Fujikawa T, Lee S, Lord CC, Ahmed N, Lee CE, Holland WL, Liu C, et al. (2018). POMC neurons expressing leptin receptors coordinate metabolic responses to fasting via suppression of leptin levels. Elife, 7.

Challis BG, Pritchard LE, Creemers JW, Delplanque J, Keogh JM, Luan J, Wareham NJ, Yeo GS, Bhattacharyya S, Froguel P, et al. (2002). A missense mutation disrupting a dibasic prohormone processing site in pro-opiomelanocortin (POMC) increases susceptibility to early-onset obesity through a novel molecular mechanism. Hum. Mol. Genet. 11, 1997–2004. [PubMed: 12165561]

Chopra AR, Louet JF, Saha P, An J, Demayo F, Xu J, York B, Karpen S, Finegold M, Moore D, et al. (2008). Absence of the SRC-2 coactivator results in a glycogenopathy resembling Von Gierke's disease. Science 322, 1395–1399. [PubMed: 19039140]

Chopra AR, Kommagani R, Saha P, Louet JF, Salazar C, Song J, Jeong J, Finegold M, Viollet B, DeMayo F, et al. (2011). Cellular energy depletion resets whole-body energy by promoting coactivator-mediated dietary fuel absorption. Cell Metab. 13, 35–43. [PubMed: 21195347]

Claret M, Smith MA, Batterham RL, Selman C, Choudhury AI, Fryer LG, Clements M, Al-Qassab H, Heffron H, Xu AW, et al. (2007). AMPK is essential for energy homeostasis regulation and glucose sensing by POMC and AgRP neurons. J Clin Invest 117, 2325–2336. [PubMed: 17671657]

Creemers JW, Lee YS, Oliver RL, Bahceci M, Tuzcu A, Gokalp D, Keogh J, Herber S, White A, O'Rahilly S, and Farooqi IS (2008). Mutations in the amino-terminal region of proopiomelanocortin (POMC) in patients with early-onset obesity impair POMC sorting to the regulated secretory pathway. J. Clin. Endocrinol. Metab. 93, 4494–4499. [PubMed: 18697863]

Dasgupta S, and O'Malley BW (2014). Transcriptional coregulators: emerging roles of SRC family of coactivators in disease pathology. J. Mol. Endocrinol. 53, R47–R59. [PubMed: 25024406]

Dietrich MO, Zimmer MR, Bober J, and Horvath TL (2015). Hypothalamic Agrp neurons drive stereotypic behaviors beyond feeding. Cell 160, 1222–1232. [PubMed: 25748653]

Duerrschmid C, He Y, Wang C, Li C, Bournat JC, Romere C, Saha PK, Lee ME, Phillips KJ, Jain M, et al. (2017). Asprosin is a centrally acting orexigenic hormone. Nat Med 23, 1444–1453. [PubMed: 29106398]

Duteil D, Chambon C, Ali F, Malivindi R, Zoll J, Kato S, Geny B, Chambon P, and Metzger D (2010). The transcriptional coregulators TIF2 and SRC-1 regulate energy homeostasis by modulating mitochondrial respiration in skeletal muscles. Cell Metab. 12, 496–508. [PubMed: 21035760]

Elmquist JK, Elias CF, and Saper CB (1999). From lesions to leptin: hypothalamic control of food intake and body weight. Neuron 22, 221–232. [PubMed: 10069329]

Farooqi IS, Drop S, Clements A, Keogh JM, Biernacka J, Lowenbein S, Challis BG, and O'Rahilly S (2006). Heterozygosity for a POMC-null mutation and increased obesity risk in humans. Diabetes 55, 2549–2553. [PubMed: 16936203]

Fukuda M, Jones JE, Olson D, Hill J, Lee CE, Gautron L, Choi M, Zigman JM, Lowell BB, and Elmquist JK (2008). Monitoring FoxO1 localization in chemically identified neurons. J. Neurosci. 28, 13640–13648. [PubMed: 19074037]

Grabauskas G, Wu X, Lu Y, Heldsinger A, Song I, Zhou SY, and Owyang C (2015). KATP channels in the nodose ganglia mediate the orexigenic actions of ghrelin. J. Physiol. 593, 3973–3989. [PubMed: 26174421]

He Y, Xu P, Wang C, Xia Y, Yu M, Yang Y, Yu K, Cai X, Qu N, Saito K, et al. (2020). Estrogen receptor-α expressing neurons in the ventrolateral VMH regulate glucose balance. Nat. Commun. 11, 2165. [PubMed: 32358493]

Hetherington AW, and Ranson SW (1940). Hypothalamic lesions and adiposity in the rat. Anat. Rec. 78, 149–172.

Hillebrand JJ, de Wied D, and Adan RA (2002). Neuropeptides, food intake and body weight regulation: a hypothalamic focus. Peptides 23, 2283–2306. [PubMed: 12535710]

Johnson AB, and O'Malley BW (2012). Steroid receptor coactivators 1, 2, and 3: critical regulators of nuclear receptor activity and steroid receptor modulator (SRM)-based cancer therapy. Mol. Cell. Endocrinol. 348, 430–439. [PubMed: 21664237]

Kim JD, Leyva S, and Diano S (2014). Hormonal regulation of the hypothalamic melanocortin system. Front Physiol 5, 480. [PubMed: 25538630]

Kitamura T, Feng Y, Kitamura YI, Chua SC Jr., Xu AW, Barsh GS, Rossetti L, and Accili D (2006). Forkhead protein FoxO1 mediates Agrp-dependent effects of leptin on food intake. Nat. Med. 12, 534–540. [PubMed: 16604086]

Kong D, Vong L, Parton LE, Ye C, Tong Q, Hu X, Choi B, Brüning JC, and Lowell BB (2010). Glucose stimulation of hypothalamic MCH neurons involves K(ATP) channels, is modulated by UCP2, and regulates peripheral glucose homeostasis. Cell Metab. 12, 545–552. [PubMed: 21035764]

Levin BE, Dunn-Meynell AA, and Routh VH (1999). Brain glucose sensing and body energy homeostasis: role in obesity and diabetes. Am. J. Physiol. 276, R1223–R1231. [PubMed: 10233011]

Madisen L, Zwingman TA, Sunkin SM, Oh SW, Zariwala HA, Gu H, Ng LL, Palmiter RD, Hawrylycz MJ, Jones AR, et al. (2010). A robust and high-throughput Cre reporting and characterization system for the whole mouse brain. Nat. Neurosci. 13, 133–140. [PubMed: 20023653]

Morton GJ, Cummings DE, Baskin DG, Barsh GS, and Schwartz MW (2006). Central nervous system control of food intake and body weight. Nature 443, 289–295. [PubMed: 16988703]

Neel JV (1999). The "thrifty genotype" in 1998. Nutr Rev 57, S2–9. [PubMed: 10391020]

Padilla SL, Carmody JS, and Zeltser LM (2010). Pomc-expressing progenitors give rise to antagonistic neuronal populations in hypothalamic feeding circuits. Nat. Med. 16, 403–405. [PubMed: 20348924]

Padilla SL, Reef D, and Zeltser LM (2012). Defining POMC neurons using transgenic reagents: impact of transient Pomc expression in diverse immature neuronal populations. Endocrinology 153, 1219–1231. [PubMed: 22166984]

Padilla SL, Qiu J, Soden ME, Sanz E, Nestor CC, Barker FD, Quintana A, Zweifel LS, Rønnekleiv OK, Kelly MJ, and Palmiter RD (2016). Agouti-related peptide neural circuits mediate adaptive behaviors in the starved state. Nat. Neurosci. 19, 734–741. [PubMed: 27019015]

Parton LE, Ye CP, Coppari R, Enriori PJ, Choi B, Zhang CY, Xu C, Vianna CR, Balthasar N, Lee CE, et al. (2007). Glucose sensing by POMC neurons regulates glucose homeostasis and is impaired in obesity. Nature 449, 228–232. [PubMed: 17728716]

Picard F, Géhin M, Annicotte J, Rocchi S, Champy MF, O'Malley BW, Chambon P, and Auwerx J (2002). SRC-1 and TIF2 control energy balance between white and brown adipose tissues. Cell 111, 931–941. [PubMed: 12507421]

Plum L, Lin HV, Dutia R, Tanaka J, Aizawa KS, Matsumoto M, Kim AJ, Cawley NX, Paik JH, Loh YP, et al. (2009). The obesity susceptibility gene Cpe links FoxO1 signaling in hypothalamic pro-opiomelanocortin neurons with regulation of food intake. Nat. Med. 15, 1195–1201. [PubMed: 19767734]

Romere C, Duerrschmid C, Bournat J, Constable P, Jain M, Xia F, Saha PK, Del Solar M, Zhu B, York B, et al. (2016). Asprosin, a Fasting-Induced Glucogenic Protein Hormone. Cell 165, 566–579. [PubMed: 27087445]

Saito K, He Y, Yan X, Yang Y, Wang C, Xu P, Hinton AO Jr., Shu G, Yu L, Tong Q, et al. (2016). Visualizing estrogen receptor-α-expressing neurons using a new ERα-ZsGreen reporter mouse line. Metabolism 65, 522–532. [PubMed: 26975544]

Santoro A, Campolo M, Liu C, Sesaki H, Meli R, Liu ZW, Kim JD, and Diano S (2017). DRP1 Suppresses Leptin and Glucose Sensing of POMC Neurons. Cell Metab 25, 647–660. [PubMed: 28190775]

Tang ED, Nunez G, Barr FG, and Guan KL (1999). Negative regulation of the forkhead transcription factor FKHR by Akt. The Journal of biological chemistry 274, 16741–16746. [PubMed: 10358014]

Tognoni CM, Chadwick JG Jr., Ackeifi CA, and Tetel MJ (2011). Nuclear receptor coactivators are coexpressed with steroid receptors and regulated by estradiol in mouse brain. Neuroendocrinology 94, 49–57. [PubMed: 21311177]

Tong Q, Ye CP, Jones JE, Elmquist JK, and Lowell BB (2008). Synaptic release of GABA by AgRP neurons is required for normal regulation of energy balance. Nat. Neurosci. 11, 998–1000. [PubMed: 19160495]

Varela L, and Horvath TL (2012). Leptin and insulin pathways in POMC and AgRP neurons that modulate energy balance and glucose homeostasis. EMBO Rep 13, 1079–1086. [PubMed: 23146889]

Vella KR, Ramadoss P, Lam FS, Harris JC, Ye FD, Same PD, O'Neill NF, Maratos-Flier E, and Hollenberg AN (2011). NPY and MC4R signaling regulate thyroid hormone levels during fasting through both central and peripheral pathways. Cell Metab 14, 780–790. [PubMed: 22100407]

Wang C, He Y, Xu P, Yang Y, Saito K, Xia Y, Yan X, Hinton A Jr., Yan C, Ding H, et al. (2018). TAp63 contributes to sexual dimorphism in POMC neuron functions and energy homeostasis. Nat. Commun. 9, 1544. [PubMed: 29670083]

Wang C, Zhou W, He Y, Yang T, Xu P, Yang Y, Cai X, Wang J, Liu H, Yu M, et al. (2021). AgRP neurons trigger long-term potentiation and facilitate food seeking. Transl. Psychiatry 11, 11. [PubMed: 33414382]

Xu Y, and López M (2018). Central regulation of energy metabolism by estrogens. Mol. Metab. 15, 104–115. [PubMed: 29886181]

Xu AW, Kaelin CB, Morton GJ, Ogimoto K, Stanhope K, Graham J, Baskin DG, Havel P, Schwartz MW, and Barsh GS (2005). Effects of hypothalamic neurodegeneration on energy balance. PLoS Biol. 3, e415. [PubMed: 16296893]

Xu Y, Nedungadi TP, Zhu L, Sobhani N, Irani BG, Davis KE, Zhang X, Zou F, Gent LM, Hahner LD, et al. (2011). Distinct hypothalamic neurons mediate estrogenic effects on energy homeostasis and reproduction. Cell Metab. 14, 453–465. [PubMed: 21982706]

Xu P, Cao X, He Y, Zhu L, Yang Y, Saito K, Wang C, Yan X, Hinton AO Jr., Zou F, et al. (2015). Estrogen receptor-α in medial amygdala neurons regulates body weight. J. Clin. Invest. 125, 2861–2876. [PubMed: 26098212]

Yang Y, Atasoy D, Su HH, and Sternson SM (2011). Hunger states switch a flip-flop memory circuit via a synaptic AMPK-dependent positive feedback loop. Cell 146, 992–1003. [PubMed: 21925320]

Yang Y, van der Klaauw AA, Zhu L, Cacciottolo TM, He Y, Stadler LKJ, Wang C, Xu P, Saito K, Hinton A Jr., et al. ; UK10K Consortium (2019). Steroid receptor coactivator-1 modulates the function of Pomc neurons and energy homeostasis. Nat. Commun. 10, 1718. [PubMed: 30979869]

Yaswen L, Diehl N, Brennan MB, and Hochgeschwender U (1999). Obesity in the mouse model of pro-opiomelanocortin deficiency responds to peripheral melanocortin. Nat. Med. 5, 1066–1070. [PubMed: 10470087]

Yore MA, Im D, Webb LK, Zhao Y, Chadwick JG Jr., Molenda-Figueira HA, Haidacher SJ, Denner L, and Tetel MJ (2010). Steroid receptor coactivator-2 expression in brain and physical associations with steroid receptors. Neuroscience 169, 1017–1028. [PubMed: 20678994]

York B, and O'Malley BW (2010). Steroid receptor coactivator (SRC) family: masters of systems biology. J. Biol. Chem. 285, 38743–38750. [PubMed: 20956538]

Yu K, He Y, Hyseni I, Pei Z, Yang Y, Xu P, Cai X, Liu H, Qu N, Liu H, et al. (2020). 17β-estradiol promotes acute refeeding in hungry mice via membrane-initiated ERα signaling. Mol. Metab. 42, 101053. [PubMed: 32712433]

Zhan C, Zhou J, Feng Q, Zhang JE, Lin S, Bao J, Wu P, and Luo M (2013). Acute and long-term suppression of feeding behavior by POMC neurons in the brainstem and hypothalamus, respectively. J. Neurosci. 33, 3624–3632. [PubMed: 23426689]

Zhu L, Xu P, Cao X, Yang Y, Hinton AO Jr., Xia Y, Saito K, Yan X, Zou F, Ding H, et al. (2015). The ERα-PI3K cascade in proopiomelanocortin progenitor neurons regulates feeding and glucose balance in female mice. Endocrinology 156, 4474–4491. [PubMed: 26375425]

Highlights

- SRC-2 inhibits POMC neurons to suppress energy expenditure during fasting
- SRC-2 maintains POMC responses to low glucose to trigger counterregulation
- SRC-2 in POMC neurons suppresses satiation and anxiety during refeeding
- SRC-2 in POMC neurons mediates diet-induced weight gain

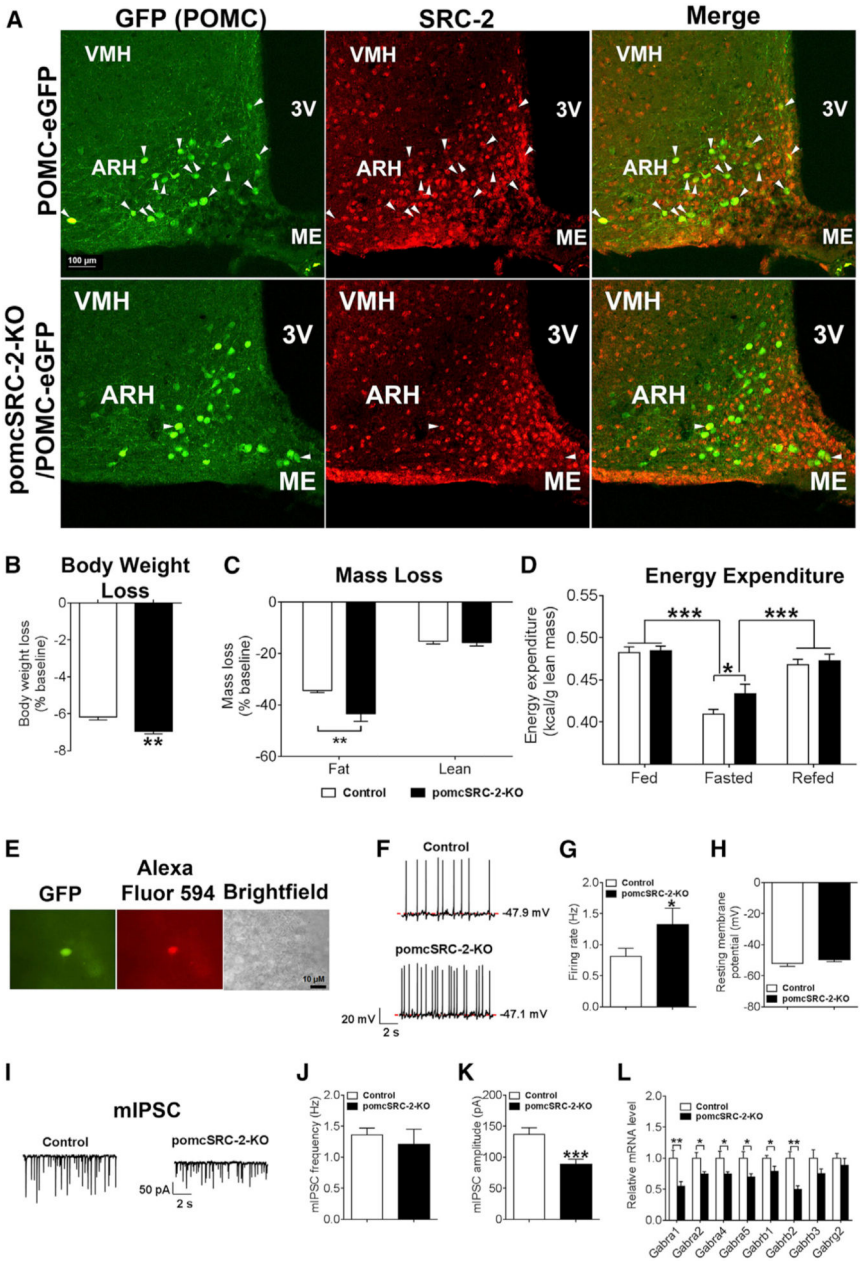

Figure 1. Deletion of SRC-2 enhances excitability of POMC neurons and increases energy expenditure during fasting

(A) Dual immunofluorescence for GFP (green) and SRC-2 (red) in the ARH of POMC-EGFP mice (controls, upper panels) and pomcSRC-2-KO/POMC-EGFP mice (lower panels). Arrowheads point to double-labeled neurons. Scale bar represents 100 μm. 3V, 3rd ventricle; ARH, arcuate nucleus of the hypothalamus; ME, median eminence; VMH, ventromedial hypothalamic nucleus.

(B and C) Changes in body weight (B), fat mass, or lean mass (C) of chow-fed male control and pomcSRC-2-KO littermates (3 to 4 months old) after a 24-h fasting. Data are presented as mean ± SEM (% baseline before fasting). n = 6 or 10 mice per group. **p < 0.01 in t tests.

(D) Daily energy expenditure measured by CLAMS in male control and pomcSRC-2-KO littermates (3 months old) during *ad libitum* fed, fasted, and refed periods. Data are presented as mean ± SEM. n = 8 or 9 mice per group. *p < 0.05 and ***p < 0.001 in two-way ANOVA analyses repeated measurement followed by Sidak tests.
(E) Representative microscopic images showing a recorded POMC neuron (GFP-labeled in POMC-EGFP mice). Scale bar represents 10 μm.
(F) Representative action potential traces in POMC neurons from fasted control versus pomcSRC-2-KO mice.
(G and H) Quantifications of firing rate (G) and resting membrane potential (H) in POMC neurons from fasted control versus pomcSRC-2-KO mice. Data are presented as mean ± SEM. n = 17 or 21 neurons from 3 mice per group. *p < 0.05 in t tests.
(I) Representative traces for mIPSC recorded in POMC neurons from fasted control versus pomcSRC-2-KO mice.
(J and K) Quantifications of frequency (J) and amplitude (K) of mIPSC. Data are presented as mean ± SEM. n = 15 or 17 neurons from 3 mice per group. *p < 0.05 in t tests.
(L) Relative mRNA levels of indicated genes measured in POMC neurons isolated from control versus pomcSRC-2-KO mice. Data are presented as mean ± SEM. n = 8 samples per group. *p < 0.05 in t tests.

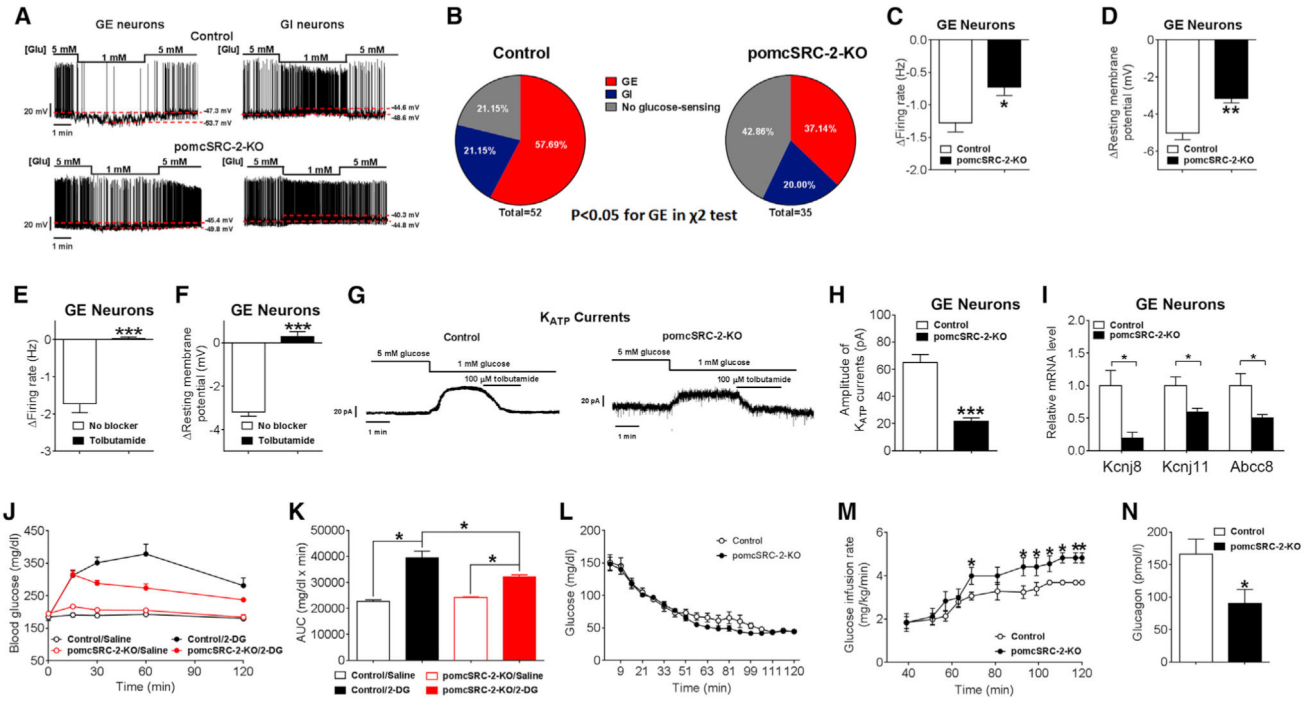

Figure 2. Deletion of SRC-2 impairs glucose sensing of POMC neurons and the counterregulatory response

(A) Representative action potential traces in response to a 5→1→5 mM glucose fluctuation in GE-POMC or GI-POMC neurons from fasted control versus pomcSRC-2-KO mice.

(B) Composition of POMC neurons from fasted control versus pomcSRC-2-KO mice that are GE, GI, or no glucose sensing. n = 52 or 35 neurons from 3 mice per group. $p < 0.05$ for GE neurons in $\chi 2$ test.

(C and D) Changes in firing rate (C) and resting membrane potential (D) in GE-POMC neurons from fasted control versus pomcSRC-2-KO mice. Data are presented as mean ± SEM. n = 13 or 30 neurons from 3 mice per group. *$p < 0.05$ and **$p < 0.01$ in t tests.

(E and F) Hypoglycemia-induced changes in firing rate (E) and resting membrane potential (F) in GE-POMC neurons from control mice in the absence or the presence of tolbutamide (100 μM). Results are presented as mean ± SEM. n = 13 neurons from 3 mice per group. ***$p < 0.001$ in t test.

(G) Representative K_{ATP} current traces in GE-POMC neurons from control versus pomcSRC-2-KO mice in response to glucose fluctuations, which were abolished by tolbutamide (100 μM).

(H) Amplitude of hypoglycemia-induced K_{ATP} currents in GE-POMC neurons from control versus pomcSRC-2-KO mice. Data are presented as mean ± SEM. n = 7 or 8 neurons from 3 mice per group. ***$p < 0.001$ in t tests.

(I) Relative mRNA levels of indicated genes measured in GE-POMC neurons isolated from control versus pomcSRC-2-KO mice. Data are presented as mean ± SEM. n = 7–12 samples per group. *$p < 0.05$ in t tests.

(J and K) Temporal blood glucose levels (J) and the area under the curves (K) measured in male control versus pomcSRC-2-KO mice (3 to 4 months old) after intraperitoneal (i.p.) injections of saline or 2-DG (500 mg/kg). Data are presented as mean ± SEM. n = 6 or 7

mice per group. *p < 0.05 in two-way ANOVA analyses repeated measurements followed by Sidak tests.

(L–N) Hyperinsulinemic-hypoglycemic clamp in male control versus pomcSRC-2-KO mice (3 to 4 months old) with matched body weight. Blood glucose (L) and glucose infusion rate (M) were measured. Data are presented as mean ± SEM. n = 5 mice per group. *p < 0.05 and **p < 0.01 in two-way ANOVA analysis repeated measurements followed by post hoc Sidak tests.

(N) Plasma glucagon levels measured at the clamped hypoglycemic condition. Data are presented as mean ± SEM. n = 5 mice per group. *p < 0.05 in t tests.

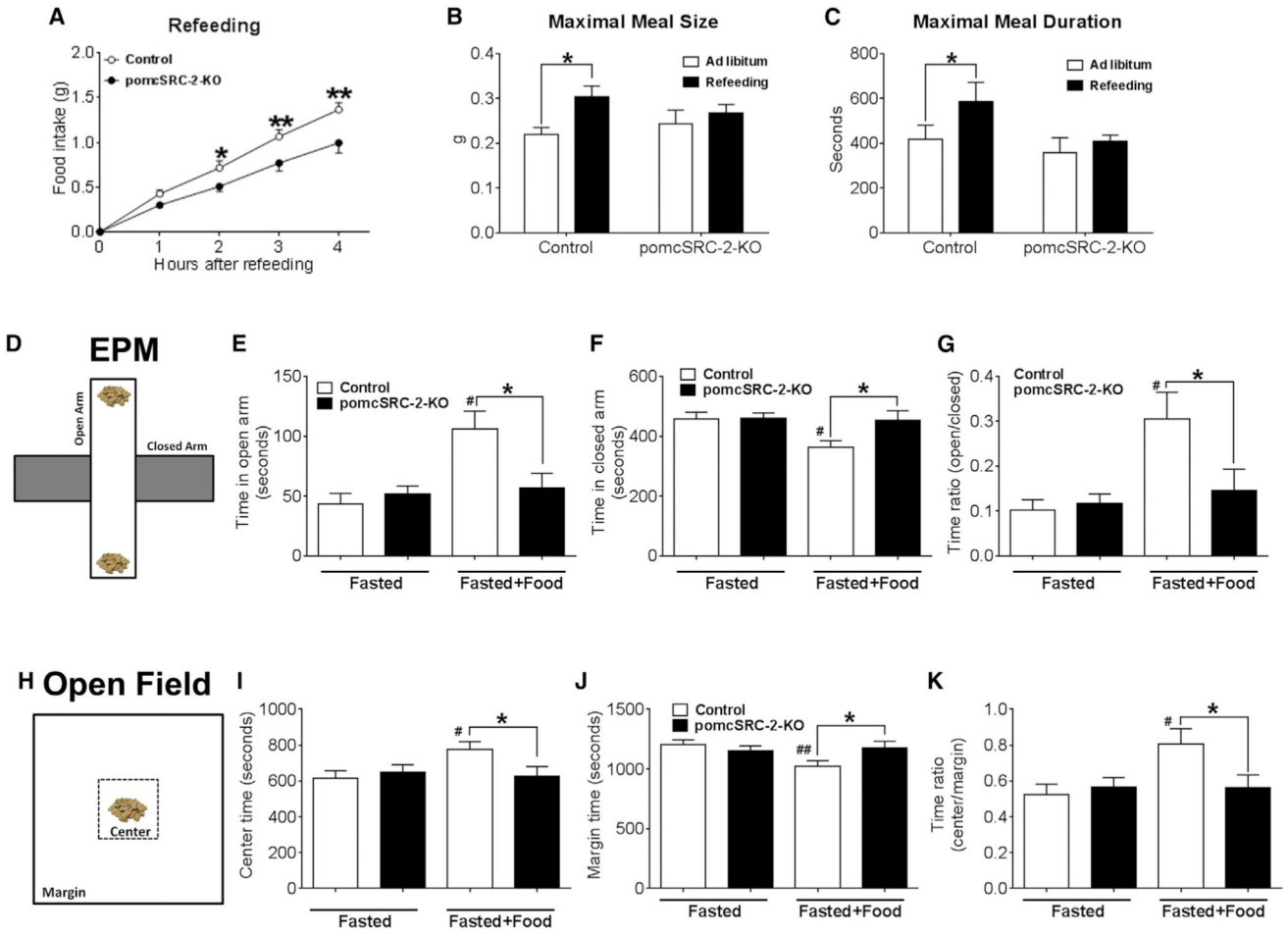

Figure 3. Deletion of SRC-2 in POMC neurons inhibits refeeding

(A) Cumulative 4-h chow refeeding after a 24-h fasting in male control and pomcSRC-2-KO littermates (4 months old). Data are presented as mean ± SEM. n = 6 or 8 mice per group. *p < 0.05 and **p < 0.01 in two-way ANOVA analyses repeated measurement followed by Sidak tests.

(B and C) Maximal meal size (B) and maximal meal duration (C) measured by CLAMS in chow-fed male control and pomcSRC-2-KO littermates (3 months old) during *ad libitum* or refeeding conditions. Data are presented as mean ± SEM. n = 7 or 9 mice per group. *p < 0.05 in two-way ANOVA analyses repeated measurement followed by Sidak tests.

(D) A schematic presentation of the elevated plus maze (EPM) with or without chow diets placed at the end of the open arms.

(E–G) Time spent in the open arms (E) and the closed arms (F) and the ratio (G) of male fasted control and pomcSRC-2-KO littermates (3 to 4 months old) with or without chow diet at the open arms. Data are presented as mean ± SEM. n = 7 or 9 mice per group. *p < 0.05 between control versus pomcSRC-2-KO; #p < 0.05 between “fasted” versus “fasted+food” within the same mouse group in two-way ANOVA analyses followed by Sidak tests.

(H) A schematic presentation of the open-field test with or without chow diets placed at the center.

(I–K) Time spent in the center (I) and the margin (J) and the ratio (K) of male fasted control and pomcSRC-2-KO littermates (3 to 4 months old) with or without chow diets at the center. Data are presented as mean ± SEM. n = 10–19 mice per group. *$p < 0.05$ between control versus pomcSRC-2-KO; #$p < 0.05$ and ##$p < 0.01$ between fasted versus fasted+food within the same mouse group in two-way ANOVA analyses followed by Sidak tests.

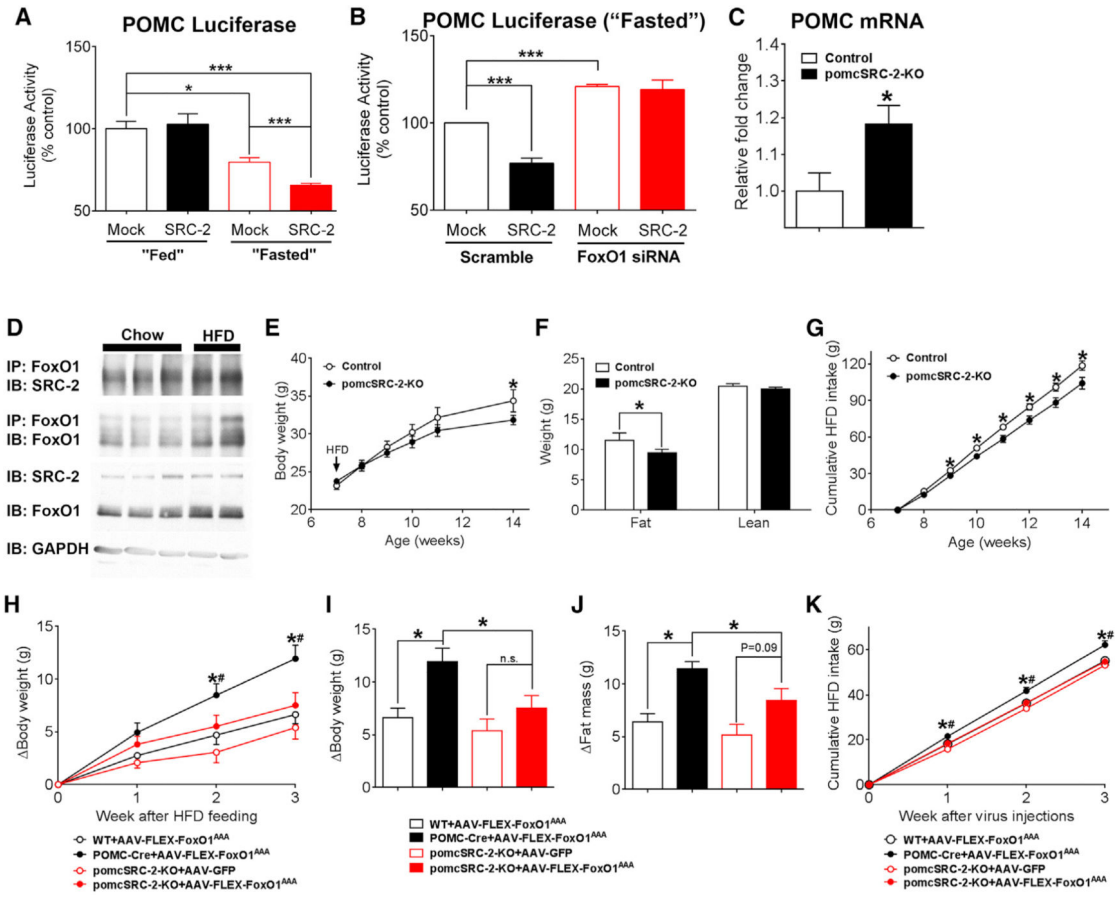

Figure 4. SRC-2 coactivates FoxO1 and mediates its energy-preserving effects

(A) Effects of SRC-2 on POMC-luciferase activity in "fed" and fasted cells. Data are presented as mean ± SEM. n = 4 or 5 repeated experiments with 6 biological replicates per group in each experiment. *p < 0.05 and ***p < 0.001 in two-way ANOVA analyses followed by Sidak tests.

(B) Effects of SRC-2 on POMC-luciferase activity in fasted cells with or without FoxO1 knockdown. Data are presented as mean ± SEM. n = 4–7 repeated experiments with 6 biological replicates per group in each experiment. ***p < 0.001 in two-way ANOVA analyses followed by Sidak tests.

(C) Hypothalamic mRNAs in fasted control and pomcSRC-2-KO mice. Data are presented as mean ± SEM. n = 14 or 15 mice per group. *p < 0.05 in t tests.

(D) Interaction of endogenous SRC-2 and FoxO1 in the hypothalamus from chow- or HFD-fed male mice.

(E) Body weight curves in male control and pomcSRC-2-KO littermates fed HFD *ad libitum* since 7 weeks of age. Data are presented as mean ± SEM. n = 8 mice per group. *p < 0.05 in two-way ANOVA analyses repeated measurement followed by Sidak tests.

(F) Fat or lean mass in 14-week-old male control and pomcSRC-2-KO littermates after 7 weeks HFD feeding. Data are presented as mean ± SEM. n = 8 mice per group. *p < 0.05 in t tests.

(G) Cumulative HFD intake in male control and pomcSRC-2-KO littermates fed HFD *ad libitum* since 7 weeks of age. Data are presented as mean ± SEM. n = 8 mice per group. *p < 0.05 in two-way ANOVA analyses repeated measurement followed by Sidak tests.
(H) Changes in body weight during a 3-week HFD feeding in mice receiving stereotaxic injections of AAV-FLEX-FoxO1^{AAA} or AAV-GFP into the ARH. Data are presented as mean ± SEM. n = 6–10 mice per group. * or #, p < 0.05 between POMC-Cre+ AAV-FLEX-FoxO1^{AAA} versus WT+ AAV-FLEX-FoxO1^{AAA} or versus pomcSRC-2-KO+AAV-FLEX-FoxO1^{AAA} in two-way ANOVA analyses repeated measurement followed by Sidak tests.
(I and J) Changes in body weight (I) and fat mass (J) at the end of the 3-week HFD feeding in mice described in (H). Data are presented as mean ± SEM. n = 6–10 mice per group. *p < 0.05 in two-way ANOVA analyses followed by Sidak tests; p = 0.09 in t tests.
(K) Cumulative HFD intake in mice described in (H). Data are presented as mean ± SEM. n = 6–10 mice per group. * or #, p < 0.05 between POMC-Cre+ AAV-FLEX-FoxO1^{AAA} versus WT+ AAV-FLEX-FoxO1^{AAA} or versus pomcSRC-2-KO+AAV-FLEX-FoxO1^{AAA} in two-way ANOVA analyses repeated measurement followed by Sidak tests.

KEY RESOURCES TABLE

REAGENT or RESOURCE	SOURCE	IDENTIFIER
Antibodies		
rabbit anti-SRC-2 antibody	Bethyl Laboratories, Inc.	#A300-345A; PRID: AB_185561
rabbit anti-SRC-2 antibody	Abcam	#ab10491; AB_297230
chicken anti-GFP antibody	Aves Labs, Inc.	#GFP-1020; AB_10000240
chicken anti-TH antibody	Abcam	#ab76442; AB_1524535
mouse monoclonal anti-Flag-HRP	Sigma	A8592; AB_439702
mouse monoclonal anti-β-Actin-HRP	Cell Signaling	#12262; AB_2566811
rabbit monoclonal anti-FoxO1 antibody	Cell Signaling	#2880; AB_2106495
mouse monoclonal anti-FoxO1 antibody	Cell Signaling	#97635; AB_2800285
Bacterial and virus strains		
AAV-FLEX-FoxO1^{AAA}-GFP	This paper	N/A
Chemicals, peptides, and recombinant proteins		
Tolbutamide	Sigma	T0891
2-Deoxy-D-glucose	Sigma	D8375
Critical commercial assays		
Single Cell-to-CT qRT-PCR Kit	Ambion, Life Technologies	4458237
Corticosterone ELISA kit	Enzo Life Sciences	ADI-900-097
Luciferase Assay Kit	Promega	E1500
Experimental models: cell lines		
HEK293	ATCC	CRL-1573
Embryonic Mouse Hypothalamus Cell Line N46	Cellutions Biosystems Inc.	CLU138
Experimental models: organisms/strains		
POMC-Cre transgenic mice	Balthasar et al., 2004	N/A
SRC-2lox/lox mice	Picard et al., 2002	N/A
POMC-eGFP mouse	Parton et al., 2007	N/A
Rosa26-LSL-tdTOMATO mouse	Madisen et al., 2010	N/A
AgRP-IRES-Cre	Tong et al., 2008	N/A
ERα-ZsGreen mice	Saito et al., 2016	N/A
AgRP-IRES-Cre/Rosa26-LSL-tdTOMATO mice	This paper	N/A
pomcSRC-2-KO/POMC-eGFP mice	This paper	N/A
POMC-Cre/Rosa26-LSL-tdTOMATO	This paper	N/A
pomc-SRC-2-KO/Rosa26-LSL-tdTOMATO	This paper	N/A
pomcSRC-2-KO mice	This paper	N/A
Oligonucleotides		

REAGENT or RESOURCE	SOURCE	IDENTIFIER
Primers for qPCR, see Table S1	This paper	N/A
Primers for luciferase reporters, see Table S2	This paper	N/A
FoxO1 siRNA (mouse-specific)	Cell Signaling	#6468
control siRNA	Cell Signaling	#6568
Recombinant DNA		
pAAV-FLEX-FoxO1AAA-GFP	This paper	N/A
pcDNA3.1-hERα	Yang et al., 2019	N/A
pCMV-FLAG-hAR	a gift from Elizabeth Wilson, Addgene, Bai et al., 2005	# 89080
pGL3-Pomc-Luciferase reporter	This paper	N/A
pGL3-Gabra1-Luciferase reporter	This paper	N/A
pGL3-Gabra2-Luciferase reporter	This paper	N/A
pGL3-Gabra4-Luciferase reporter	This paper	N/A
pGL3-Gabra5-Luciferase reporter	This paper	N/A
pGL3-Gabrb1-Luciferase reporter	This paper	N/A
pGL3-Gabrb2-Luciferase reporter	This paper	N/A
pGL3-Abcc8-Luciferase reporter	This paper	N/A
pGL3-Kcnj8-Luciferase reporter	This paper	N/A
pGL3-Kcnj11-Luciferase reporter	This paper	N/A